

Nonlinear Aerodynamics of a Delta Wing in Combined Pitch and Roll

J. Er-El,* D. Seter,† and D. Weihs‡

Technion—Israel Institute of Technology, Haifa, Israel

This paper presents an experimental study on the effects of roll on the loading and rolling moment of a 60 deg swept delta wing. The parameters studied were the incidence angle (including those in which vortex breakdown was present), roll angle, and ground proximity. Results indicate that when vortex breakdown is not present, the effects of roll on the wing loading and rolling moment are in reasonable agreement with predictions. When vortex breakdown is present, the magnitude of the rolling moment coefficient is reduced considerably and its sign can even be altered. The changes in the rolling moment characteristics due to vortex breakdown can be attributed to the roll-induced spanwise displacement of the leading-edge vortices. Effects of ground proximity on roll characteristics were shown to be small.

Nomenclature

a	= parameter in the Joukowski transformation
C_N	= normal force coefficient
$C_{N,1}$	= contribution of the leading half-wing to C_N
$C_{N,2}$	= contribution of the lee half-wing to C_N
$\bar{C}_{N,1}$	= $C_{N,1}/C_N$
$\bar{C}_{N,2}$	= $C_{N,2}/C_N$
C_R	= rolling moment coefficient
c	= wing root chord
c_p	= pressure coefficient, $= (p - p_\infty)/q$
h	= height above the ground of the chordwise station $\bar{x} = \frac{2}{3}$ (see Fig. 8)
\bar{h}	= proximity ratio, $= h/s(1)$
p	= pressure
q	= dynamic pressure
$s(\bar{x})$	= wing local semispan
V_∞	= freestream velocity
W	= complex potential, $= \phi + i\psi$ (see Appendix)
\bar{x}	= nondimensional chordwise coordinate, $= x/c$
\bar{x}_{VB}	= chordwise position of vortex breakdown
\bar{y}	= nondimensional local spanwise coordinate, $= y/s(\bar{x})$
α	= angle of attack for a wing in combined pitch and roll
β	= yaw angle
Γ	= circulation of the concentrated vortex, (see Appendix)
ϵ	= $\alpha'/tg^{-1}[s(1)/c]$ (see Appendix)
ϕ	= flow potential (see Appendix)
ψ	= stream function (see Appendix)
ρ	= density
ζ	= $\xi + i\eta$ (see Fig. A1)
ϕ	= roll angle for a wing in combined pitch and roll
σ	= $y + iz$ (see Fig. A1)

Subscripts

- 1 = leading vortex
2 = lee vortex

Superscript

- () = conditions in the approximate model (see Appendix)

Introduction

COMBINED pitch and roll (or the equivalent, combined pitch and yaw) maneuvers, in addition to the classical application in takeoff and landing situations with side wind, are of importance to a highly maneuverable aircraft capable of executing controlled side slipping maneuvers. For delta-winged aircraft executing such maneuvers, the wing loading, in both the symmetrical and asymmetrical cases, is strongly influenced by the leading-edge vortices. These vortices induce suction peaks on the upper surface of the wing and thus contribute to its lift.

The contribution of these vortices for delta wings in combined pitch and yaw has been previously studied for wings having sweep angles of 75 deg¹ and 80 deg² and at angles of attack in which vortex breakdown was not present in the symmetrical case. These studies, which were based on surface pressure measurements and on flow visualizations, indicate that yaw affects both the vortex positions and the suction they induce. Due to yaw, the leading vortex is displaced inboard and downward, while the lee vortex is displaced outward and upward. The changes in vortex positions are accompanied by an increase in the vortex-induced suction peak due to the leading vortex and by a decrease in that due to the lee vortex. Both studies showed that yaw stimulates vortex breakdown of the leading vortex. The wings used in these studies were highly swept; consequently, even small yaw angles caused the lee vortex to drift outboard, off the wing, considerably reducing the induced suction.

In this paper, an experimental study of the effects of roll on the loading of a 60 deg swept delta wing is presented. For this wing, which is typical of those used in both present and future aircraft configurations, the lee vortex is not swept off the wing even at high roll or yaw angles. The parameters studied are the incidence angle, which included those in which vortex breakdown was present in the symmetrical case, the roll angle, and ground proximity. The experimental results will be compared with predictions obtained from an approximate model of the phenomenon.

Experimental Installation

The experiments were carried out in the 1 × 1 m closed, subsonic wind tunnel at the Technion Aeronautical Research Center. They consisted of detailed surface pressure measurements as well as force and moment measurements. In these experiments, the freestream speed was 32 m/s, the Reynolds number 0.6×10^6 (based on the wing root chord), and the incidence angles were 15 and 25 deg incidence. At each inci-

Received May 15, 1988; revision received Sept. 9, 1988. Copyright © 1988 American Institute of Aeronautics and Astronautics, Inc. All rights reserved.

*Senior Lecturer, Faculty of Aeronautical Engineering.

†Graduate Student, Faculty of Aeronautical Engineering.

‡Professor, Faculty of Aeronautical Engineering. Member AIAA.

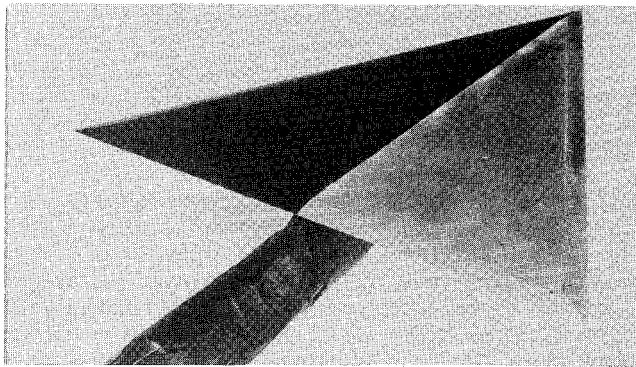


Fig. 1a Pressure measurement wing model.

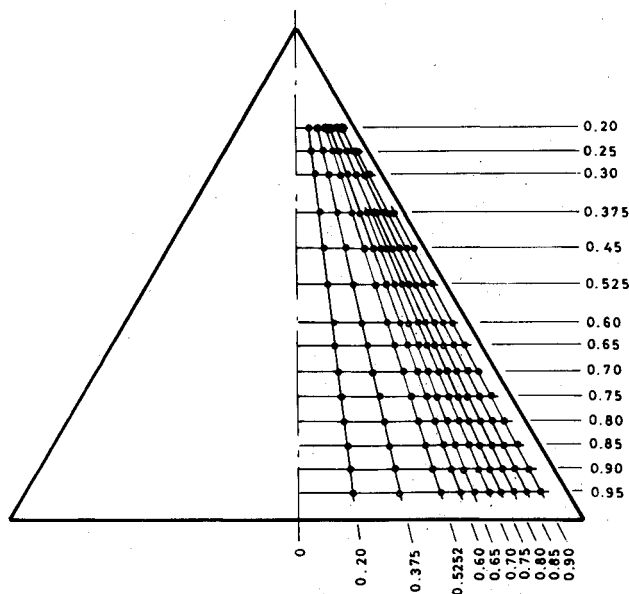


Fig. 1b Map of pressure measurement ports.

dence, measurements were taken for $\phi = 0, 15$, and 25 deg and $\bar{h} = 0.56$ and 1.76 .

The pressure measurements were carried out on a 60 deg swept delta wing model of 246 mm root chord, 4.6 mm thickness and beveled leading and trailing edges of 30 deg angle (Fig. 1a). The wing holder is attached to the lower surface, leaving the pressure measurement surface free of obstructions and resulting in a blockage factor of $\sim 0.5\%$. This and other required corrections were taken from Ref. 3. The wing is equipped with 130 pressure ports on the starboard side of the upper surface in an arrangement shown in Fig. 1b.

The pressure measurement system consists of three 48-port Scanivalve modules, each connected to a pressure transducer. The system provides the readings of the surface pressures, freestream dynamic pressure, and a calibration pressure. A detailed description of the measurement system and its accuracy is given in Refs. 4 and 5. The ground was simulated by a flat board, 1.25 cm thick and 150 cm long, having a sharp leading edge and spanning the width of the wind tunnel parallel to the wind-tunnel floor, starting approximately 100 cm upstream of the wing's leading edge (Fig. 2).

The pressure measurement procedure was dictated by the fact that the pressure ports are concentrated on one-half of the upper surface. Consequently, a complete surface pressure map for a given α and ϕ required four runs. To obtain the pressures on the upper planform, measurements were taken at the given α and ϕ for the starboard (leading) side and at α and $-\phi$ for the port (lee) side. To obtain pressures on the lower planform,

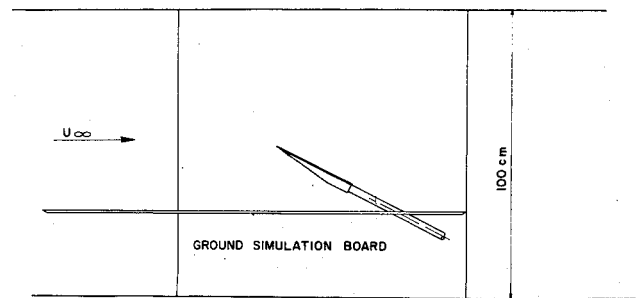


Fig. 2 General side view of the wing model and the ground board in the wind tunnel.

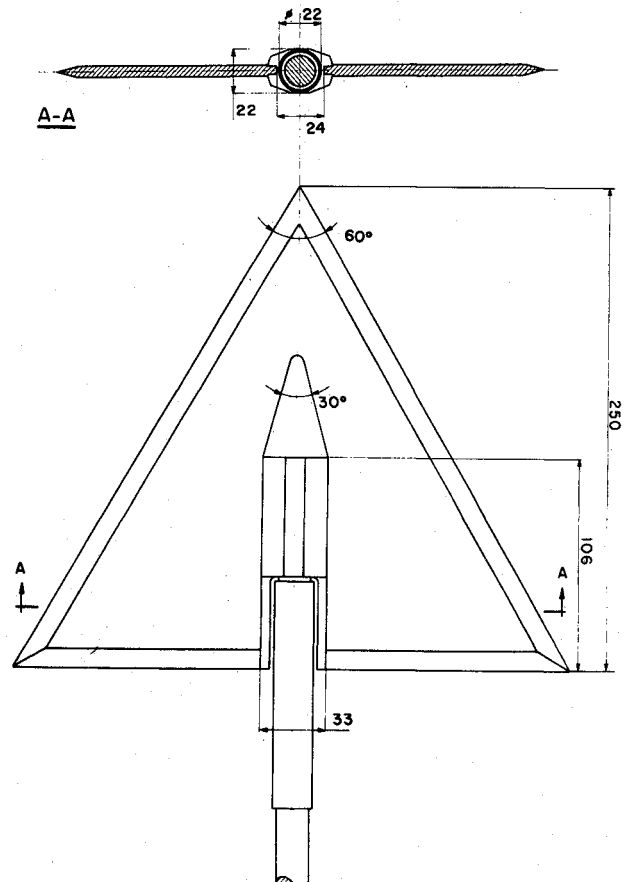


Fig. 3 Force and moment measurement model.

measurements were taken at α and $180 + \phi$ for the starboard side and at α and $180 - \phi$ for the port side.

The force and moment measurements were carried out using a six-component sting balance on a model having the same geometry as the one used for the pressure measurement, except for the wing holder (Fig. 3). The force and moment measurements were carried out under the same conditions as the surface pressures.

Results and Discussion

Figure 4 illustrates the effects of roll on the surface pressures at the upper planform for $\alpha = 15$ deg. At this incidence and for $\phi = 0$ deg, the wing is only marginally affected by vortex breakdown ($\bar{x}_{VB} \approx 0.85$).⁶ Roll affects both the position and magnitude of the vortex-induced suction peaks. The lee suction peak is displaced outward, while the leading suction peak is shifted inboard. The effects of roll on the suction peak magnitudes are influenced by vortex breakdown. In the apex region (represented by $\bar{x} = 0.38$), away from vortex breakdown effects, the magnitude of the suction induced by the leading

vortex increases, while that induced by the lee vortex decreases. In the trailing-edge region (represented by $\bar{x}=0.95$), affected by vortex breakdown, the effects of roll are reversed. In this region, the roll-related effects of vortex breakdown on the spanwise profile of the suction peaks appear to be weaker on the lee vortex and stronger on the leading one. This indicates that for positive roll, the position of vortex breakdown on the leading vortex moves upstream, while that on the lee vortex moves downstream.

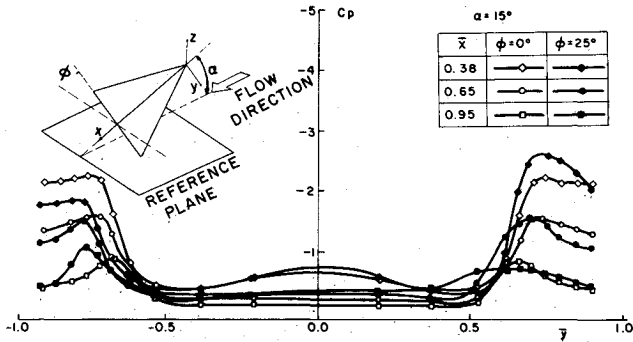


Fig. 4 Effect of roll on the pressures at the upper surface, $\alpha = 15$ deg.

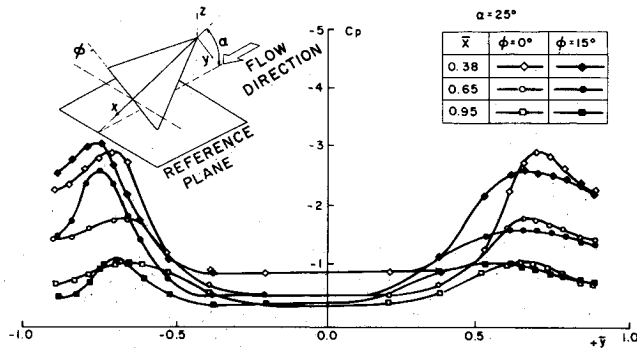


Fig. 5 Effect of roll on the pressures at the upper surface, $\alpha = 25$ deg.

Figure 5 features the surface pressures at $\alpha = 25$ deg for $\phi = 0$ and 15 deg. For $\phi = 0$ deg, $\bar{x}_{VB} \approx 0.25$,⁶ and thus all spanwise c_p profiles shown for this roll angle are affected by vortex breakdown. In this case, the magnitude of the lee suction peak increases and its spanwise profile appears to become less affected by vortex breakdown. Thus, the weaker effects of vortex breakdown on this vortex, as observed for this incidence angle and for the trailing-edge region at $\alpha = 15$ deg (Fig. 4), resulted in increased suction. On the other hand, the effects of vortex breakdown on the spanwise profile of the leading vortex become more pronounced with roll and the magnitude of the suction peak decreases. Examination of the position of the suction peaks indicates that their spanwise displacement due to roll has a similar trend to that observed for $\alpha = 15$ deg.

Figure 6 features the effects of a further increase of ϕ from 15 to 25 deg at $\alpha = 25$ deg. The additional rolling angle resulted in a further displacement of the suction peaks in the same direction as that observed in Fig. 5 and a reduction of the magnitude of those suction peaks. The reduction in the magnitude of the leading suction peak, which appears to be affected by vortex breakdown for these roll angles, is similar to that observed for this angle in Fig. 5. The reduction in the magnitude of the lee suction peak, which appears to be less affected by vortex breakdown for these roll angles is similar to that observed for this vortex at $\alpha = 15$ deg in the region unaffected by vortex breakdown. This indicates that when the vortex is

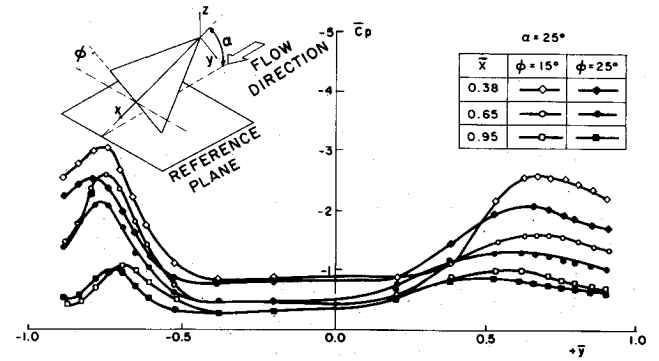


Fig. 6 Effect of roll on the pressures at the upper surface, $\alpha = 25$ deg.

Table 1 Predicted effects of roll on the leading-edge vortices

α	ϕ	Lee vortex				Leading vortex			
		$\bar{y}(\phi)$	$\bar{z}(\phi)$	$\Gamma(\phi)$	$\bar{p}, \min(\phi)$	$\bar{y}(\phi)$	$\bar{z}(\phi)$	$\Gamma(\phi)$	$\bar{p}, \min(\phi)$
		$\bar{y}(\phi=0)$	$\bar{z}(\phi=0)$	$\Gamma(\phi=0)$	$\bar{p}, \min(\phi=0)$	$\bar{y}(\phi=0)$	$\bar{z}(\phi=0)$	$\Gamma(\phi=0)$	$\bar{p}, \min(\phi=0)$
15	15	1.006	1.008	0.916	0.845	0.998	0.927	0.999	1.143
	25	1.012	0.975	0.827	0.749	0.999	0.848	0.952	1.231
25	15	1.018	1.032	0.896	0.779	0.989	0.910	1.017	1.225
	25	1.033	1.018	0.790	0.637	0.987	0.824	0.976	1.367

Table 2 Effects of roll and ground proximity on C_N and C_R

α	ϕ	$C_N(\phi)$		C_R		Ground effect			
		$C_N(\phi=0)$				$\bar{C}_{N,2}$ $\bar{C}_{N,1}$		$C_N(\bar{h}=0.56)$ $C_R(\bar{h}=0.56)$	
		Measured	Predicted	Measured	Predicted			$C_N(\bar{h}=1.76)$	$C_R(\bar{h}=1.76)$
15	15	0.96	0.97	-0.044	-0.031	0.47	0.53	1.06	1.07
	25	0.89	0.89	-0.91	-0.047	0.45	0.55	1.06	1.28
25	15	0.94	0.96	0.010	-0.091	0.47	0.53	1.07	2.46
	25	0.83	0.91	0.002	-0.137	0.45	0.55	1.12	3.11

unaffected by vortex breakdown, an increase in the roll angle results in a decrease in the suction peak induced by it.

Some of the above features are also evident in predictions obtained from an approximate model developed for a delta wing in pitch and yaw (see Appendix), based on the model by Brown and Michael.⁷ Although this model neglects vortex breakdown, it provides an indication and an explanation for some of the effects of roll on the aerodynamics of the wing. Table 1 presents the predicted effects of roll on the vortices' positions, circulations, and the suction they induce on the wing for the conditions at which the measurements were taken (the coordinate transformation from the pitch and yaw conditions of the approximate model to the pitch and roll conditions of the experimental data is given in the Appendix). The predictions show that due to roll, the leading vortex is displaced downward and marginally inboard, its circulation remains approximately unchanged, and the suction it induces on the wing increases. On the other hand, the lee vortex is only marginally displaced (in both the spanwise and vertical directions), while the circulation as well as the induced suction decreases. Thus, the increased suction of the leading vortex can be attributed to its increased proximity to the wing surface (since its circulation is unchanged), while the decreased suction of the lee vortex is a consequence of the decreased circulation (since its vertical position is virtually unchanged). Comparison of the predicted effects of roll on the suction peaks with the measured results (Figs. 4–6) shows a qualitative agreement only when the vortices are free of vortex breakdown effects. This is evident in Fig. 4 for the upstream region of the wing (represented by $\bar{x} = 0.38$) and in Fig. 6 for the lee vortex. However, the predicted results may also indicate that the enhancement of vortex breakdown effects due to increased roll observed experimentally on the leading vortex in Figs. 4–6, are caused by the decrease in its height due to roll.

The rolling angle effects on the lower surface are marginal. This is highlighted in Fig. 7, which shows both that the magni-

tudes of c_p on this surface are small and that the variations due to roll are miniscule.

The effects of ground proximity on the pressures at the suction surface of the banked wing are presented in Fig. 8. The ground-free case is represented by $h = 1.76$ (at this height, ground proximity effects have been shown⁵ to be negligible for the wing used) and the ground-affected case is represented by $h = 0.56$. Results indicate that ground proximity increases the suction induced by the leading-edge vortices in a manner similar to that observed in Ref. 5 for a wing in pure pitch ($\phi = 0$ deg).

Integral Characteristics

Both the experimental and predicted results pertaining to the roll-induced effects on the wing loading are shown in Table 2. These results indicate that roll reduces the normal force acting on the wing. For $\alpha = 15$ deg, the measured reduction is similar to the predicted one, whereas at $\alpha = 25$ deg, where vortex breakdown effects are significant, the measured reduction is larger than predicted.

The asymmetric, roll-induced loading is evident in the difference in the normal force contributions $\bar{C}_{N,1}$ and $\bar{C}_{N,2}$ of the two wing halves. These contributions were computed by numerical integration of the measured surface pressures in a manner described in Refs. 4 and 5. In the present study, $\bar{C}_{N,1}$ is consistently larger than $\bar{C}_{N,2}$ for positive roll angles, even though roll enhances the vortex breakdown effects on the leading half and attenuated them on the lee half.

Examination of the rolling moment indicates that, at $\alpha = 15$ deg, both the experimental and predicted coefficients are negative and decrease with increasing roll angle. At $\alpha = 25$ deg, the predicted coefficients are also negative and show the same trends as those at $\alpha = 15$ deg, while the measured values are positive. The deviation of the measured C_R at $\alpha = 25$ deg from that measured at $\alpha = 15$ deg and from the predictions can be analyzed in view of the fact that the wing rolling moment is a balance between the positive sign contribution of the leading half-wing and the negative one of the lee half. The contribution of each half is the product of the normal force acting on it and the distance from its center of pressure to the rolling axis. Roll has two counteracting effects on the rolling moment of each wing half. On the leading half, roll increases the proportional share of the normal force, but reduces the distance from its center of pressure to the rolling axis by displacing the vortex induced suction peak inboard. On the lee side, the roll effects are opposite. Since the roll-induced effects on $\bar{C}_{N,1}$ and $\bar{C}_{N,2}$ are similar at both $\alpha = 15$ and 25 deg, it can be deduced that the source of the wide variations in the measured C_R is the roll-induced displacement of the centers of pressure of these two halves. At $\alpha = 15$ deg, the negative C_R is consistent with a small displacement, whereas at $\alpha = 25$ deg, the positive C_R indicates increased displacement, sufficient to alter the direction of the rolling moment. The increased displacement at $\alpha = 25$ deg is probably a consequence of vortex breakdown, which affects the leading-edge vortices at this angle.

Summary

The present study illustrates the influence of vortex breakdown on the rolling moment characteristics. For the 60 deg swept delta wing, from which the leading-edge vortices are not swept off even at high roll angles, the presence of vortex breakdown reduces the magnitude of $\partial C_R / \partial \phi$ considerably and even alters its sign. This result should be taken into account when considering limits of maneuverability for aircraft with such wings.

Appendix

The approximate model used in the present study utilizes the approach proposed by Brown and Michael.⁷ In this approach, it is assumed that the wing is slender and the flow about it is

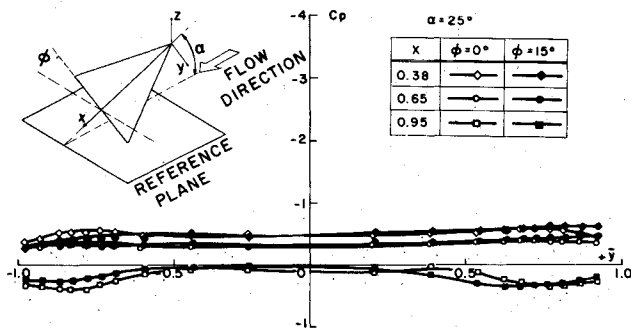


Fig. 7 Effect of roll on the pressure at the lower surface, $\alpha = 28$ deg.

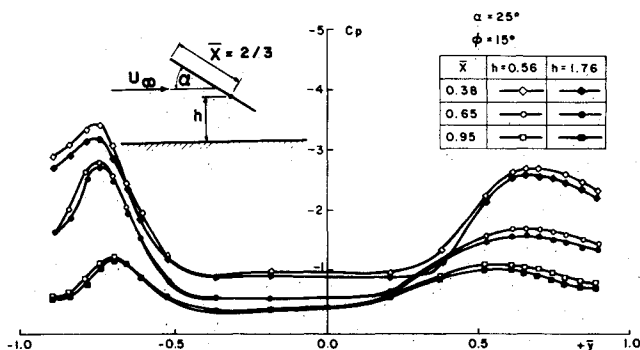


Fig. 8 Effect of ground proximity on the pressure at the upper surface ($\alpha = 25$ deg, $\phi = 15$ deg).

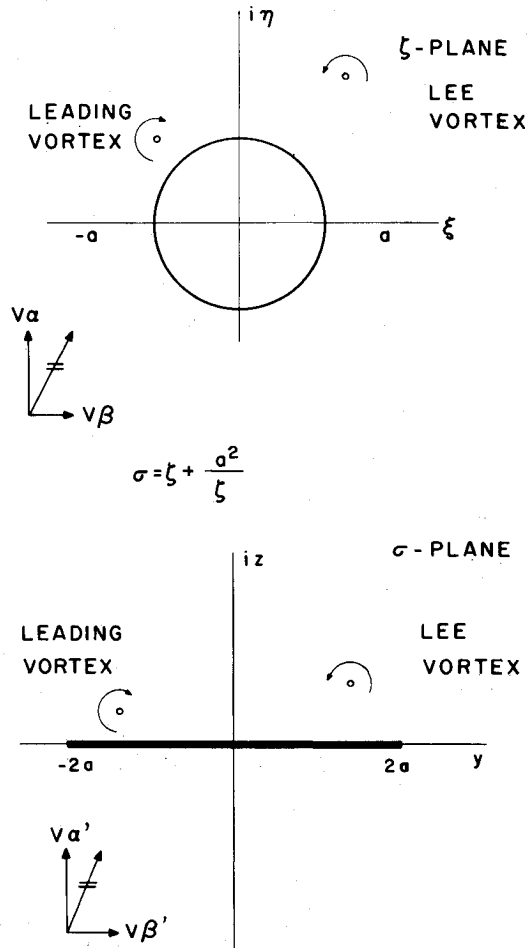


Fig. A1 Crossflow plane.

conical. The cross flow is governed by the two-dimensional Laplace equation in the y - z planes. The two leading-edge vortices are represented as two concentrated vortices, each connected to the leading edge by a feeding vortex sheet. The positions and the circulation of the vortices are determined from the requirements that the flow velocity at the leading edge is finite (Kutta condition) and that the force acting on each vortex/feeding sheet system is zero.

In the present model, the flow in the cross plane is a flow with uniform sideslip about a plate and two vortices. The complex potential $W(\sigma)$ describing this flow is obtained by a Joukowski transformation of the flow about a cylinder and two vortices (Fig. A1), as

$$\begin{aligned}
 W(\sigma) = & -\frac{i\Gamma_1}{2\pi} \ln \left(\frac{\sigma + \sqrt{\sigma^2 - 4a^2}}{2} - \zeta_1 \right) \\
 & -\frac{i\Gamma_2}{2\pi} \ln \left(\frac{\sigma + \sqrt{\sigma^2 - 4a^2}}{2} - \zeta_2 \right) \\
 & -iV\alpha' \left(\frac{\sigma + \sqrt{\sigma^2 - 4a^2}}{2} - \frac{2a^2}{\sigma + \sqrt{\sigma^2 - 4a^2}} \right) \\
 & -iV\beta' \left(\frac{\sigma + \sqrt{\sigma^2 - 4a^2}}{2} - \frac{2a^2}{\sigma + \sqrt{\sigma^2 - 4a^2}} \right)
 \end{aligned} \quad (A1)$$

The Kutta condition gives the following relation:

$$\begin{aligned}
 \frac{i\Gamma_1}{2\pi} \left(\frac{1}{a - \zeta_1} - \frac{1}{a - \frac{a^2}{\zeta_1}} \right) + \frac{i\Gamma_2}{2\pi} \left(\frac{1}{a - \zeta_2} - \frac{1}{a - \frac{a^2}{\zeta_2}} \right) \\
 + i \cdot V\alpha' \cdot 2 = 0
 \end{aligned} \quad (A2a)$$

$$\begin{aligned}
 \frac{i\Gamma_1}{2\pi} \left(\frac{1}{a + \zeta_1} - \frac{1}{a + \frac{a^2}{\zeta_1}} \right) + \frac{i\Gamma_2}{2\pi} \left(\frac{1}{a + \zeta_2} - \frac{1}{a + \frac{a^2}{\zeta_2}} \right) \\
 - i \cdot V\alpha' \cdot 2 = 0
 \end{aligned} \quad (A2b)$$

while from the zero force condition, we get

$$i \cdot \rho \cdot \Gamma_1 \left[-V_1^* + V \cdot \epsilon \cdot \left(\frac{2\sigma_1 - 2a}{2a} \right) \right] = 0 \quad (A3a)$$

$$i \cdot \rho \cdot \Gamma_2 \left[-V_2^* + V \cdot \epsilon \cdot \left(\frac{2\sigma_2 - 2a}{2a} \right) \right] = 0 \quad (A3b)$$

where

$$V_1^* = \left(\frac{\bar{\sigma}_1}{a} - 1 \right) \cdot V \cdot \epsilon \quad (A4a)$$

$$V_2^* = \left(\frac{\bar{\sigma}_2}{a} + 1 \right) \cdot V \cdot \epsilon \quad (A4b)$$

Equations (A2-A4) determine the position and circulation of both leading-edge vortices.

The pressure distribution is determined from

$$p = p_\infty - \frac{1}{2}\rho V^2 \left(\frac{2\varphi_x}{V} + \frac{\varphi_y^2}{V^2} + \frac{\varphi_z^2}{V^2} - \alpha^2 \right) \quad (A5)$$

the normal force is obtained from

$$L = -\rho V \operatorname{Real} \left(\oint W(\zeta) \frac{d\sigma}{d\zeta} d\zeta \right) \quad (A6)$$

and the rolling moment is given by

$$\begin{aligned}
 M_R = & \frac{\rho}{2} \left\{ V \cdot \operatorname{Real} \left[\oint W(\sigma) d(\sigma\bar{\sigma}) \right] \right. \\
 & \left. + \operatorname{Real} \left[\int_0^c dx \oint \left(\frac{dw}{d\sigma} \right)^2 \sigma d\sigma \right] \right\}
 \end{aligned} \quad (A7)$$

where c is a contour enclosing the plate and two vortices.

Although this model was developed for a wing in pitch and yaw (with no roll), it can also be utilized for a wing in equivalent pitch and roll (with no yaw) after transformation of the coordinate system using the following relations:

$$\begin{aligned}
 V'_\infty &= V_\infty \cdot \cos \alpha \\
 \alpha' &= tg \alpha \cdot \cos \phi \\
 \beta' &= -tg \alpha \cdot \sin \phi
 \end{aligned} \quad (A8)$$

Acknowledgment

The authors would like to thank Mr. Asaf Levin for his assistance in developing the approximate model.

References

¹Harvey, J. K., "Some Measurements on a Yawed Slender Delta Wing with Leading-Edge Separation," British Aeronautical Research Council, R&M 3160, 1961.

²Hummel, D., "Untersuchungen über das Aufplatzen der Wirbel an Schlanken Deltaflügeln," *Zeitschrift für Flugwissenschaften*, Vol. 13, No. 5, 1965, pp. 155-168.

³Borovik, Y., "Subsonic Wind Tunnel Wall Corrections," M.Sc. Thesis, Technion, Haifa, Israel, 1975.

⁴Er-El, J., "Effect of Wing/Canard Interference on the Loading of a Delta Wing," *Journal of Aircraft*, Vol. 25, Jan. 1988, pp. 18-24.

⁵Er-El, J. and Weihs, D., "Ground Effect on Slender Wings Moderate and High Angles of Attack," ICAS Paper 84.2.8.2, Sept. 1984. (also *Journal of Aircraft*, Vol. 23, May 1986, pp. 357-358.)

⁶Wentz, W. J., Jr. and Kohlman, D. L., "Wind Tunnel Investigation of Vortex Breakdown on Slender Sharp-Edged Wings," Research Center, University of Kansas, Lawrence, Rept. FRL-68-013, 1968.

⁷Brown, C. E. and Michael, W. H., "On Slender Delta Wings with Leading-Edge Separation," NACA TN 3430, 1955.

*Recommended Reading from the AIAA
Progress in Astronautics and Aeronautics Series . . .*



Single- and Multi-Phase Flows in an Electromagnetic Field: Energy, Metallurgical and Solar Applications

Herman Branover, Paul S. Lykoudis, and Michael Mond, editors

This text deals with experimental aspects of simple and multi-phase flows applied to power-generation devices. It treats laminar and turbulent flow, two-phase flows in the presence of magnetic fields, MHD power generation, with special attention to solar liquid-metal MHD power generation, MHD problems in fission and fusion reactors, and metallurgical applications. Unique in its interface of theory and practice, the book will particularly aid engineers in power production, nuclear systems, and metallurgical applications. Extensive references supplement the text.

TO ORDER: Write AIAA Order Department,
370 L'Enfant Promenade, S.W., Washington, DC 20024

Please include postage and handling fee of \$4.50 with all orders.
California and D.C. residents must add 6% sales tax. All foreign orders
must be prepaid. Please allow 4-6 weeks for delivery. Prices are subject
to change without notice.

1985 762 pp., illus. Hardback
ISBN 0-930403-04-5

AIAA Members \$59.95

Nonmembers \$89.95

Order Number V-100